

Fastener Modeling for Joining Composite Parts

*Alexander Rutman, Chris Boshers – Spirit AeroSystems
Larry Pearce, John Parady – MSC.Software Corporation*

2009 Americas Virtual Product Development Conference
April 21-22, 2009
Phoenix, AZ

Abstract

The finite element modeling techniques of fastener joints is described in detail in previous papers of the authors [1, 2]. However, these papers addressed only the fasteners joining metallic parts. The continued trend is to use more composite materials in aircraft structures. The finite element analysis of such structures requires modeling of fastener joints connecting composite parts, metallic parts, or combination of the two.

The work presented in this paper extends the fastener FEM formulation previously developed for metallic parts to enable its use with composite parts. The main difference between modeling of fasteners in metallic and composite parts is in the interface between the fastener and the part. In composite parts the bearing stiffness depends on the direction of the fastener reaction. Because of this, the problem becomes non-linear and requires a number of iterations to solve it. At every iteration, the bearing stiffness in the fastener – composite part interface should be updated. The presented procedure describes this iterative process which can be used with any number of fasteners joining composite and metallic parts. This modeling techniques is described in terms of MSC.Nastran but can be extended to other FE codes.

1. Introduction.

Development of the finite element modeling techniques presented in this paper was dictated by widening usage of composite materials in aircraft structures. The modeling techniques of fastener joints developed earlier [1, 2] was dedicated to metallic parts. Modeling of fasteners joining composite parts requires a different approach to the interface between fastener and joined composite part. In joints of metallic parts, the bearing stiffness of the joint does not depend on the direction of the fastener reaction because of isotropy of the joined materials. In joints of composite parts, the joined materials possess anisotropic or orthotropic properties. This means that the bearing stiffness in the fastener – composite part interface used in the finite element model depends on direction of the fastener reaction. This phenomenon can influence the distribution of loads between fasteners in the joint.

This problem is therefore non-linear, and requires a number of iterations to solve it. After every iteration the fastener reactions change their directions and bearing stiffnesses at fastener – composite parts interfaces should be recalculated. The procedure must be

repeated until the process converges. This paper explains in detail the iterative process of the finite element analysis of a structure containing fasteners joining composite parts. The described iterative process in this paper is illustrated by numerical example.

The presented procedure can be used with any number of composite and metallic joint members. However, the composite members can be modeled only by shell elements. Metallic members can be modeled by both shell and solid elements. The modeling technique is described in terms of MSC.Nastran but can be extended to other FE codes. The presented procedure is supported by an MSC.Patran PCL utility created by MSC.Software Corporation.

2. Modeling Configurations.

The fastener finite element modeling approach is described in detail in [1, 2]. Examples of fastener joint models are shown in Figure 1.

The joined parts can be modeled either by shell or solid elements [2]. The shell elements can be used for both metallic and composite parts. The solid elements can be used only for metallic parts.

Idealization of a plate-fastener system includes the following:

- Bending and shear stiffness of a fastener shank;
- Elastic bearing stiffness of a plate and fastener at the contact surface;
- Compatibility of displacements of a fastener and connected plates in the joint.

The fastener shank is modeled by CBAR or CBEAM elements [3] with corresponding PBAR or PBEAM cards for properties definition.

The interaction between a fastener and plates results in bearing deformation of all components of the joint on their surfaces of contact. The combined bearing stiffness of a fastener and connected plates is defined in Section 3 for composite parts and in Section 4 for metallic parts. The bearing stiffness is presented as a translational stiffness in the direction of axes normal to the fastener axis which define the fastener shear plane, and rotational stiffness about the same axes. The bearing stiffnesses are modeled by CBUSH elements [3] (springs in examples in Figure 1) or by combinations of CELAS2 elements. When the plate is modeled by shell elements, the load from the CBUSH element is transferred directly to the shell elements. In the case of the plate modeled by solid elements, load from the CBUSH element node located in the plate mid plane is transferred to the solid elements nodes by a rigid element RBE2 (grey arrows in examples in Figure 1).

Modeling of compatibility of displacements in the joint can be performed by two ways:

1. Modeling using only rigid elements (see examples in Figure 1).
2. Modeling using rigid elements and linear gap technique. This modeling approach is described in [2].

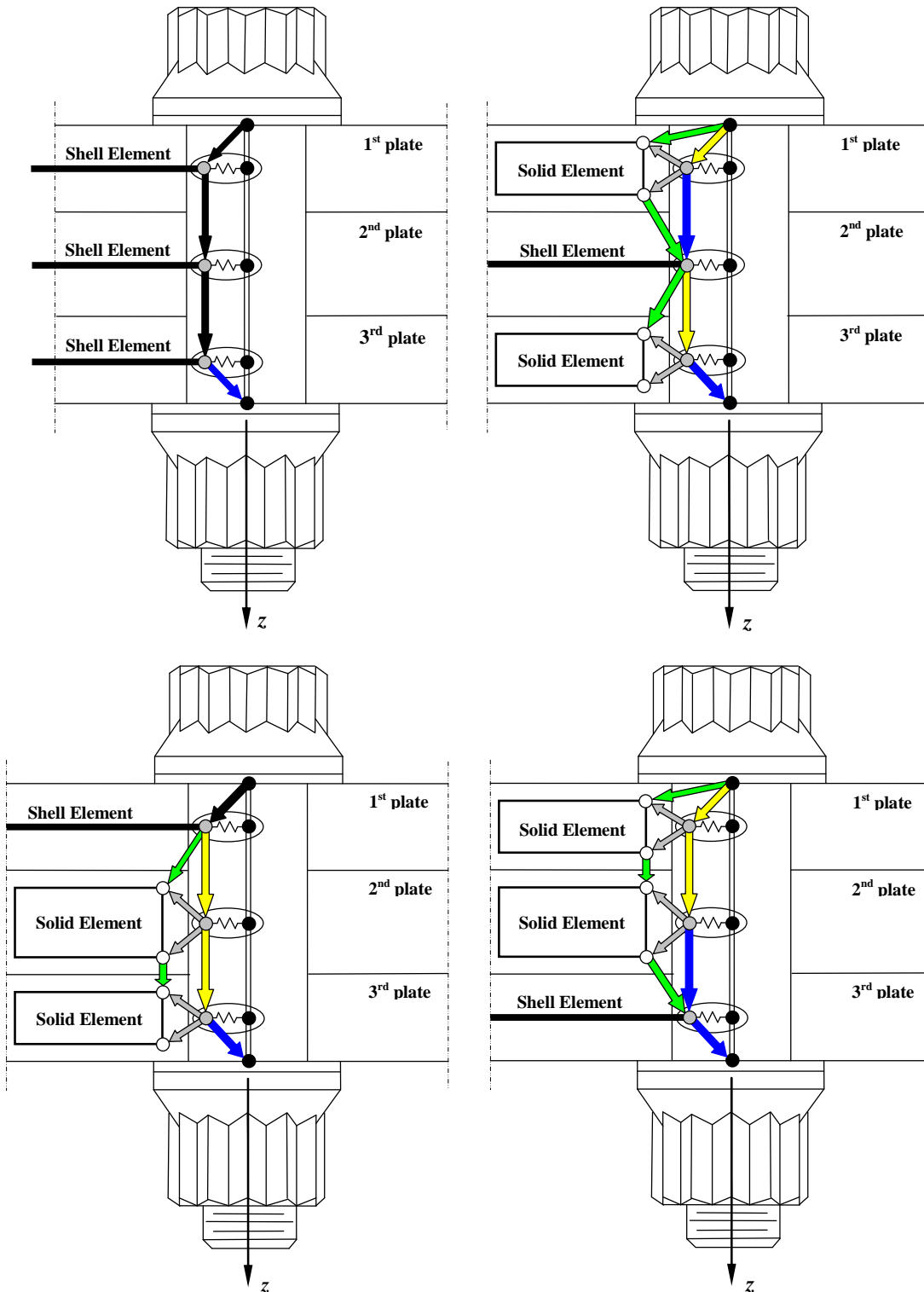


Figure 1. Examples of Fastener Joint Models.

The fastener joint is modeled under the following assumptions:

- No interference of plates under the load;
- The plate mid-planes stay parallel to each other under load;
- Planes under the fastener heads stay parallel to the plate mid-planes under load.

For the first modeling method these goals are reached by using two sets of RBAR elements.

The first set of RBAR elements (black and green arrows in Figure 1) satisfies the first assumption. These RBAR elements prevent the movement of plates relative to each other along the fastener axis.

The second set of RBAR elements (black, blue, and yellow arrows in Figure 1) satisfies the last two assumptions. It forces the plate mid-planes and planes under the fastener heads to remain parallel to each other under load.

Two sets of RBAR elements are required when the joint connects the plates modeled by solid elements because solid elements do not have rotational stiffness at their nodes. When all joined plates are modeled by shell elements, all required degrees of freedom can be assigned to one set of rigid elements.

More detail explanation of modeling technique for compatibility of displacement in the joint is given in [2].

3. Bearing Stiffness in Composite Part – Fastener Interface.

3.1. Translational Bearing Stiffness

3.1.1. Translational bearing flexibility of ply i of the composite plate in directions x and y (Figure 2) of the fastener coordinate system

$$C_{ixbtp} = \frac{1}{\bar{Q}_{11}^{(i)} t_i} = \frac{1}{\bar{Q}_{11}^{(i)} (z_i - z_{i-1})} \quad (1-a)$$

$$C_{iybtp} = \frac{1}{\bar{Q}_{22}^{(i)} t_i} = \frac{1}{\bar{Q}_{22}^{(i)} (z_i - z_{i-1})} \quad (1-b)$$

where t_i - ply i thickness;

$$t_i = z_i - z_{i-1}$$

z_i - coordinate of ply i upper surface;

z_{i-1} - coordinate of ply i lower surface.

Components of the transformed reduced stiffness matrix [4, 5]:

$\bar{Q}_{11}^{(i)}$ - transformed reduced stiffness for ply i in the x -direction

$$\bar{Q}_{11}^{(i)} = Q_{11}^{(i)} m_i^4 + 2(Q_{12}^{(i)} + 2Q_{66}^{(i)}) m_i^2 n_i^2 + Q_{22}^{(i)} n_i^4 \quad (2)$$

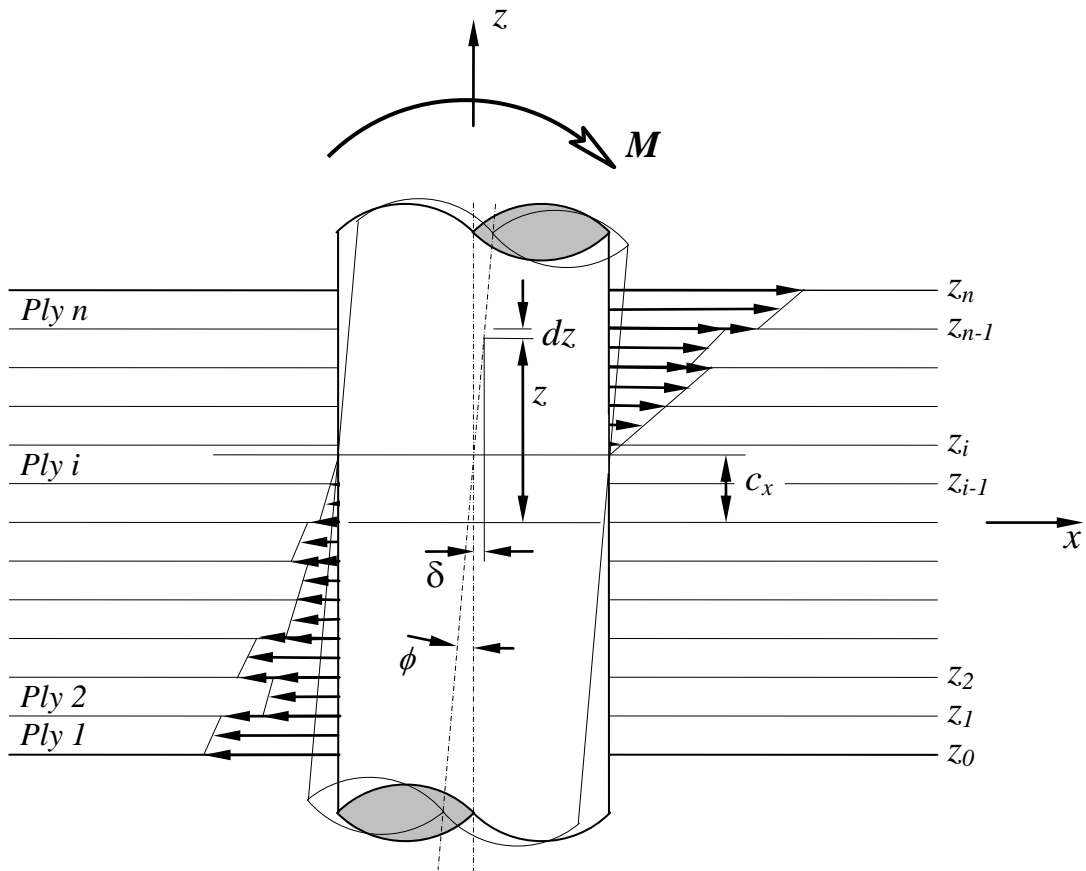


Figure 2. Rotational Bearing Stiffness Definition.

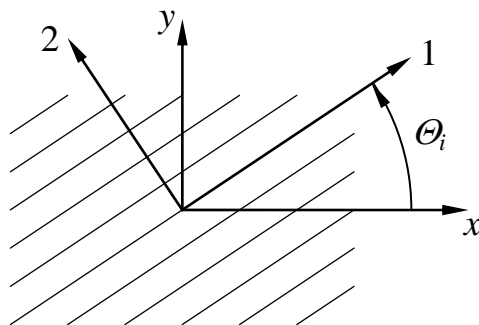


Figure 3. Material Principal Axes 1-2 for Ply i and the Fastener Coordinate System x - y .

$\bar{Q}_{22}^{(i)}$ - transformed reduced stiffness for ply i in the y -direction

$$\bar{Q}_{22}^{(i)} = Q_{11}^{(i)} n_i^4 + 2(Q_{12}^{(i)} + 2Q_{66}^{(i)}) m_i^2 n_i^2 + Q_{22}^{(i)} m_i^4 \quad (3)$$

In formulas (2) and (3) above

$Q_{11}^{(i)}, Q_{12}^{(i)}, Q_{22}^{(i)}, Q_{66}^{(i)}$ - components of the reduced stiffness matrix for ply i

$$m_i = \cos \theta_i \quad \text{and} \quad n_i = \sin \theta_i \quad (4)$$

where θ_i - angle of ply i orientation (Figure 3)

The reduced stiffness matrix for ply i

$$Q^{(i)} = \begin{bmatrix} Q_{11}^{(i)} & Q_{12}^{(i)} & 0 \\ Q_{12}^{(i)} & Q_{22}^{(i)} & 0 \\ 0 & 0 & Q_{66}^{(i)} \end{bmatrix} \quad (5)$$

Non-zero components of reduced stiffness matrix for ply i

$$Q_{11}^{(i)} = \frac{E_1^{(i)}}{1 - \nu_{12}^{(i)} \nu_{21}^{(i)}} \quad Q_{22}^{(i)} = \frac{E_2^{(i)}}{1 - \nu_{12}^{(i)} \nu_{21}^{(i)}} \quad (6)$$

$$Q_{12}^{(i)} = \frac{\nu_{12}^{(i)} E_2^{(i)}}{1 - \nu_{12}^{(i)} \nu_{21}^{(i)}} = \frac{\nu_{21}^{(i)} E_1^{(i)}}{1 - \nu_{12}^{(i)} \nu_{21}^{(i)}} \quad Q_{66}^{(i)} = G_{12}^{(i)}$$

The engineering constants in expressions (6) are

$E_1^{(i)}, E_2^{(i)}$ - Elastic moduli of ply i in material principal 1 and 2 directions respectively (Figure 3);

$G_{12}^{(i)}$ - Shear modulus in the lamina i plane (plane 1-2);

$\nu_{12}^{(i)}$ - Poisson's ratio in the lamina i plane;

$$\nu_{21}^{(i)} = \nu_{12}^{(i)} \frac{E_2^{(i)}}{E_1^{(i)}}$$

3.1.2. Translational bearing flexibility of the fastener at ply i location (Figure 2)

$$C_{ixbtf} = C_{iybtf} = \frac{1}{E_{cf} t_i} = \frac{1}{E_{cf} (z_i - z_{i-1})} \quad (7)$$

where E_{cf} - compression modulus of fastener material.

3.1.3. Combined translational bearing flexibility of the joint at ply i location in directions x and y

Summation of expressions (1-a) and (1-b) with expression (7) gives

$$C_{ixbt} = C_{ixbtp} + C_{ixbtf} = \frac{1}{\overline{Q}_{11}^{(i)} t_i} + \frac{1}{E_{cf} t_i} = \frac{1}{t_i} \left(\frac{1}{\overline{Q}_{11}^{(i)}} + \frac{1}{E_{cf}} \right) \quad (8-a)$$

$$C_{iybt} = C_{iybtp} + C_{iybtf} = \frac{1}{\overline{Q}_{22}^{(i)} t_i} + \frac{1}{E_{cf} t_i} = \frac{1}{t_i} \left(\frac{1}{\overline{Q}_{22}^{(i)}} + \frac{1}{E_{cf}} \right) \quad (8-b)$$

3.1.4. Combined translational bearing stiffness of the joint at ply i location in directions x and y

After reversing expressions (8-a) and (8-b)

$$S_{ixbt} = \frac{1}{C_{ixbt}} = \frac{t_i}{\frac{1}{\overline{Q}_{11}^{(i)}} + \frac{1}{E_{cf}}} \quad (9-a)$$

$$S_{iybt} = \frac{1}{C_{iybt}} = \frac{t_i}{\frac{1}{\overline{Q}_{22}^{(i)}} + \frac{1}{E_{cf}}} \quad (9-b)$$

3.1.5. Combined translational bearing stiffness at composite plate with the fastener contact (these values should be defined for every composite plate in the joint)

After summation of bearing stiffnesses of plies

$$S_{xbt} = \sum_{i=1}^n S_{ixbt} = \sum_{i=1}^n \frac{t_i}{\frac{1}{\overline{Q}_{11}^{(i)}} + \frac{1}{E_{cf}}} \quad (10-a)$$

$$S_{ybt} = \sum_{i=1}^n S_{iybt} = \sum_{i=1}^n \frac{t_i}{\frac{1}{\overline{Q}_{22}^{(i)}} + \frac{1}{E_{cf}}} \quad (10-b)$$

where n - number of plies in the composite plate.

3.2. Rotational Bearing Stiffness

3.2.1. Composite plate neutral axes

Neutral axis coordinate in plane normal to axis x

$$c_x = \frac{\sum_{i=1}^n S_{ixbt} \cdot \frac{z_i + z_{i-1}}{2}}{S_{xbt}}$$

Similar, neutral axis coordinate in plane normal to axis y

$$c_y = \frac{\sum_{i=1}^n S_{iybt} \cdot \frac{z_i + z_{i-1}}{2}}{S_{ybt}}$$

After substitution of expressions (9-a) and (9-b) for S_{ixbt} and S_{iybt} into formulae for c_x and c_y above

$$c_x = \frac{\sum_{i=1}^n \frac{z_i - z_{i-1}}{\frac{1}{\overline{Q}_{11}^{(i)}} + \frac{1}{E_{cf}}} \cdot \frac{z_i + z_{i-1}}{2}}{S_{xbt}} = \frac{1}{2} \cdot \frac{\sum_{i=1}^n \frac{z_i^2 - z_{i-1}^2}{\frac{1}{\overline{Q}_{11}^{(i)}} + \frac{1}{E_{cf}}}}{S_{xbt}} \quad (11-a)$$

$$c_y = \frac{\sum_{i=1}^n \frac{z_i - z_{i-1}}{\frac{1}{\overline{Q}_{22}^{(i)}} + \frac{1}{E_{cf}}} \cdot \frac{z_i + z_{i-1}}{2}}{S_{ybt}} = \frac{1}{2} \cdot \frac{\sum_{i=1}^n \frac{z_i^2 - z_{i-1}^2}{\frac{1}{\overline{Q}_{22}^{(i)}} + \frac{1}{E_{cf}}}}{S_{ybt}} \quad (11-b)$$

3.2.2. Rotational bearing deformation

The relative rotation of the plate and fastener creates a moment in the plate fastener interaction. The bearing deformations caused by this relative rotation are assumed distributed linearly along the plate thickness (Figure 2).

Bearing deformations in x -direction

$$\delta_x = \phi_x (z - c_x) \quad (12-a)$$

Bearing deformations in y -direction

$$\delta_y = \phi_y (z - c_y) \quad (12-b)$$

Here ϕ_x - angle of the fastener and plate relative rotation in plane x - z ;

ϕ_y - angle of the fastener and plate relative rotation in plane y - z .

3.2.3. Bearing flexibilities of a dz thick slice of ply i of the composite plate

Bearing flexibility of the slice in direction x

$$dC_{ixbrp} = \frac{1}{\overline{Q}_{11}^{(i)}} dz \quad (13-a)$$

Bearing flexibility of the slice in direction y

$$dC_{iybrp} = \frac{1}{\overline{Q}_{22}^{(i)}} dz \quad (13-b)$$

3.2.4. Bearing flexibility of the fastener at a dz thick slice of ply i location

$$dC_{ixbrf} = dC_{iybrf} = \frac{1}{E_{cf} dz} \quad (14)$$

3.2.5. Combined bearing flexibility of the composite plate and fastener at a dz thick slice of ply i location

Summation of flexibilities of a dz thick slice of the plate ply (equations 13-a and 13-b) and the fastener (equation 14) gives combined bearing flexibility in directions x and y

$$dC_{ixbr} = dC_{ixbrp} + dC_{ixbrf} = \frac{1}{dz} \left(\frac{1}{\overline{Q}_{11}^{(i)}} + \frac{1}{E_{cf}} \right) \quad (15-a)$$

$$dC_{iybr} = dC_{iybrp} + dC_{iybrf} = \frac{1}{dz} \left(\frac{1}{\overline{Q}_{22}^{(i)}} + \frac{1}{E_{cf}} \right) \quad (15-b)$$

3.2.6. Combined bearing stiffness of the composite plate and fastener at a dz thick slice of ply i location

Reversing equations 15-a and 15-b gives combined bearing stiffnesses in directions x and y

$$dS_{ixbr} = \frac{1}{dC_{ixbr}} = \frac{dz}{\frac{1}{\overline{Q}_{11}^{(i)}} + \frac{1}{E_{cf}}} \quad (16-a)$$

$$dS_{iybr} = \frac{1}{dC_{iybr}} = \frac{dz}{\frac{1}{\overline{Q}_{22}^{(i)}} + \frac{1}{E_{cf}}} \quad (16-b)$$

3.2.7. Load at plate-fastener contact at dz thick slice of ply i location caused by combined bearing deformation.

Load in direction x

$$dF_{ix} = \delta_x dS_{ixbr}$$

After substitution of expressions 12-a and 16-a into the above

$$dF_{ix} = \frac{\phi_x}{\frac{1}{\overline{Q}_{11}^{(i)}} + \frac{1}{E_{cf}}} (z - c_x) dz \quad (17-a)$$

Similarly, load in direction y

$$dF_{iy} = \delta_y dS_{iybr}$$

and after substitution of (12-b) and (16-b)

$$dF_{iy} = \frac{\phi_y}{\frac{1}{\overline{Q}_{22}^{(i)}} + \frac{1}{E_{cf}}} (z - c_y) dz \quad (17-b)$$

3.2.8. Moments of dF_{ix} and dF_{iy} forces about neutral axes

Taking (17-a) and (17-b) into account moment of load dF_{ix}

$$dM_{ix} = (z - c_x) dF_{ix} = \frac{\phi_x}{\frac{1}{\overline{Q}_{11}^{(i)}} + \frac{1}{E_{cf}}} (z - c_x)^2 dz \quad (18-a)$$

and moment of load dF_{iy}

$$dM_{iy} = (z - c_y) dF_{iy} = \frac{\phi_y}{\frac{1}{\overline{Q}_{22}^{(i)}} + \frac{1}{E_{cf}}} (z - c_y)^2 dz \quad (18-b)$$

3.2.9. Moments of ply i loads about neutral axes

Moment of load F_{ix}

$$\begin{aligned} M_{ix} &= \int_{z_{i-1}}^{z_i} dM_{ix} = \phi_x \int_{z_{i-1}}^{z_i} \frac{1}{\left(\frac{1}{\overline{Q}_{11}^{(i)}} + \frac{1}{E_{cf}} \right)} (z - c_x)^2 dz \\ &= \frac{\phi_x}{3} \cdot \frac{1}{\frac{1}{\overline{Q}_{11}^{(i)}} + \frac{1}{E_{cf}}} \cdot \left[(z_i - c_x)^3 - (z_{i-1} - c_x)^3 \right] \end{aligned} \quad (19-a)$$

Moment of load F_{iy}

$$\begin{aligned} M_{iy} &= \int_{z_{i-1}}^{z_i} dM_{iy} = \phi_y \int_{z_{i-1}}^{z_i} \frac{1}{\left(\frac{1}{\overline{Q}_{22}^{(i)}} + \frac{1}{E_{cf}} \right)} (z - c_y)^2 dz \\ &= \frac{\phi_y}{3} \cdot \frac{1}{\frac{1}{\overline{Q}_{22}^{(i)}} + \frac{1}{E_{cf}}} \cdot \left[(z_i - c_y)^3 - (z_{i-1} - c_y)^3 \right] \end{aligned} \quad (19-b)$$

3.2.10. Moments in plate-fastener contact caused by bearing

After summation through all the plies

$$M_x = \sum_{i=1}^n M_{ix} = \frac{\phi_x}{3} \sum_{i=1}^n \frac{(z_i - c_x)^3 - (z_{i-1} - c_x)^3}{\frac{1}{\bar{Q}_{11}^{(i)}} + \frac{1}{E_{cf}}} \quad (20-a)$$

$$M_y = \sum_{i=1}^n M_{iy} = \frac{\phi_y}{3} \sum_{i=1}^n \frac{(z_i - c_y)^3 - (z_{i-1} - c_y)^3}{\frac{1}{\bar{Q}_{22}^{(i)}} + \frac{1}{E_{cf}}} \quad (20-b)$$

3.2.11. Rotational bearing stiffness in plate-fastener contact

$$S_{xbr} = \frac{M_x}{\phi_x} = \frac{1}{3} \sum_{i=1}^n \frac{(z_i - c_x)^3 - (z_{i-1} - c_x)^3}{\frac{1}{\bar{Q}_{11}^{(i)}} + \frac{1}{E_{cf}}} \quad (21-a)$$

$$S_{ybr} = \frac{M_y}{\phi_y} = \frac{1}{3} \sum_{i=1}^n \frac{(z_i - c_y)^3 - (z_{i-1} - c_y)^3}{\frac{1}{\bar{Q}_{22}^{(i)}} + \frac{1}{E_{cf}}} \quad (21-b)$$

4. Bearing Stiffness in Metallic Part – Fastener Interface.

4.1. Translational Bearing Stiffness

Assuming in formulae (6)

$$E_1 = E_2 = E, \quad G_{12} = G = \frac{E}{2(1+\nu)} \quad \text{and} \quad \nu_{12} = \nu_{21} = \nu$$

the reduced stiffness matrix components for metallic (isotropic) part are

$$Q_{11} = Q_{22} = \frac{E}{1-\nu^2} \quad Q_{12} = \frac{\nu E}{1-\nu^2} \quad Q_{66} = G = \frac{E}{2(1+\nu)}$$

Components of the transformed reduced stiffness matrix are

$$\bar{Q}_{11} = \bar{Q}_{22} = \frac{E}{1-\nu^2} \quad (22)$$

In the above expressions:

E – elastic compression modulus of metallic part;

G – shear modulus;

ν – Poisson's ratio.

The translational bearing stiffness of the metallic plate is

$$S_{xbrp} = S_{ybrp} = \frac{E t}{1-\nu^2} \quad (23)$$

where t – thickness of metallic plate.

In the earlier publications [1, 2] another expression was used for the translational bearing stiffness of metallic plate

$$S_{x_{btp}} = S_{y_{btp}} = E t \quad (24)$$

These two expressions for translational bearing stiffness of the metallic plate were verified by the finite element method. The model for the translational bearing stiffness definition is shown in Figure 4.

The model material has the following properties:

Elastic Modulus	$E = 10.3 \text{ msi}$
Poisson's Ratio	$\nu = 0.33$
Model Thickness	$t = 0.1 \text{ in}$

The model is constrained along the line through the center of the circular hole (Figure 4).

The model is loaded by force $P = 1000 \text{ lbs}$ applied in the center of the hole (Figure 5). From the center of the hole the load is transferred to the hole edge by RBE2 elements defined in cylindrical coordinate system.

Displacement of the plate center under the load $w = 8.383135E-4 \text{ in}$

Translational bearing stiffness of the plate obtained by the finite element analysis

$$S_{btp(FEM)} = \frac{P}{w} = \frac{1000}{0.0008383135} = 1,192,871 \text{ lb/in}$$

Comparison of translational bearing stiffnesses obtained by the finite element analysis with analyses using formulae (23) and (24) are given in Table 1.

It can be seen from the table that formula (23) gives the better result.

The combined translational bearing stiffness at metallic plate with the fastener contact

$$S_{x_{bt}} = S_{y_{bt}} = \frac{t}{\frac{1-\nu^2}{E} + \frac{1}{E_{cf}}} \quad (25)$$

4.2. Rotational Bearing Stiffness

Following similar considerations the combined rotational bearing stiffness at metallic plate with the fastener contact will be

$$S_{x_{br}} = S_{y_{br}} = \frac{1}{12} \cdot \frac{t^3}{\frac{1-\nu^2}{E} + \frac{1}{E_{cf}}} \quad (26)$$

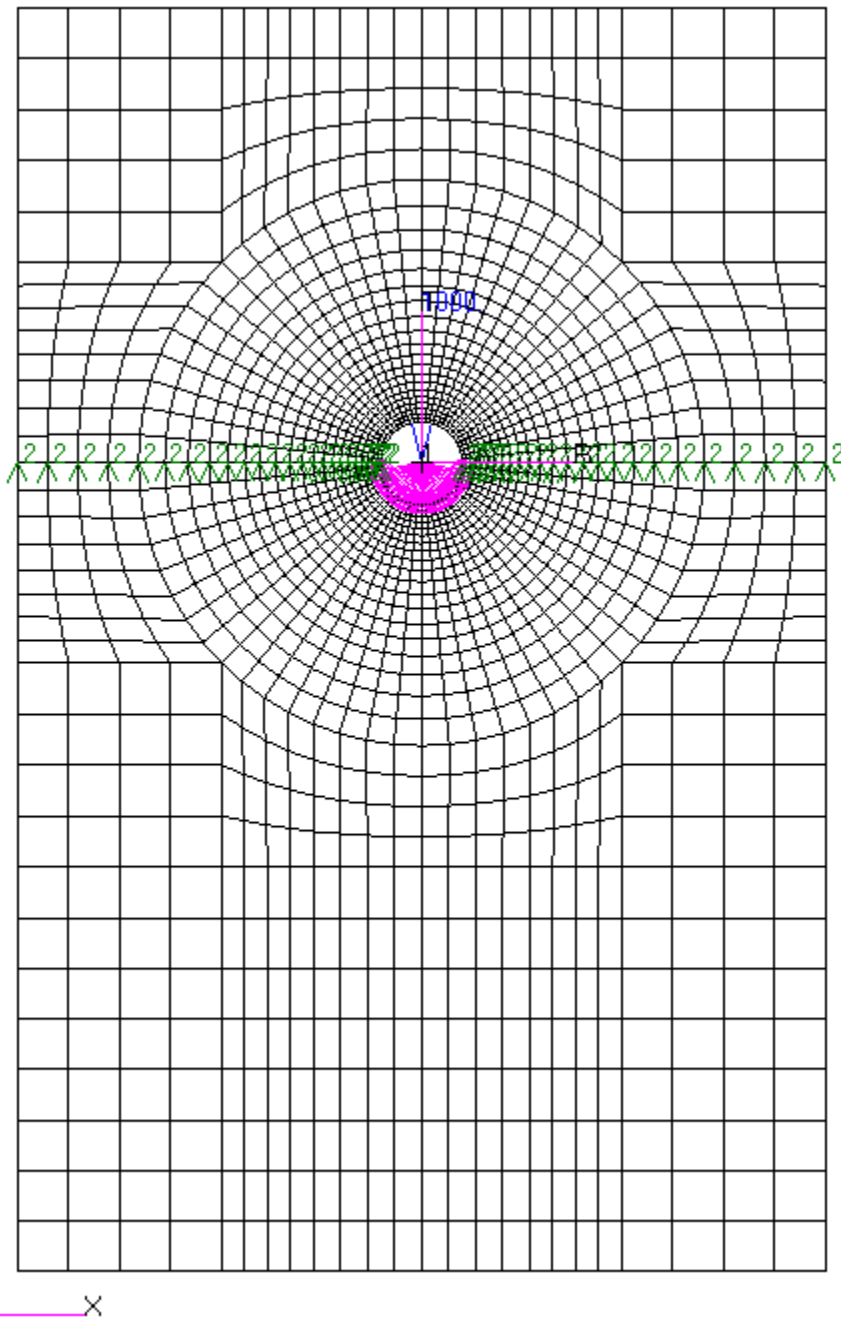


Figure 4. Finite Element Model for Metallic Plate Translational Bearing Stiffness Definition.

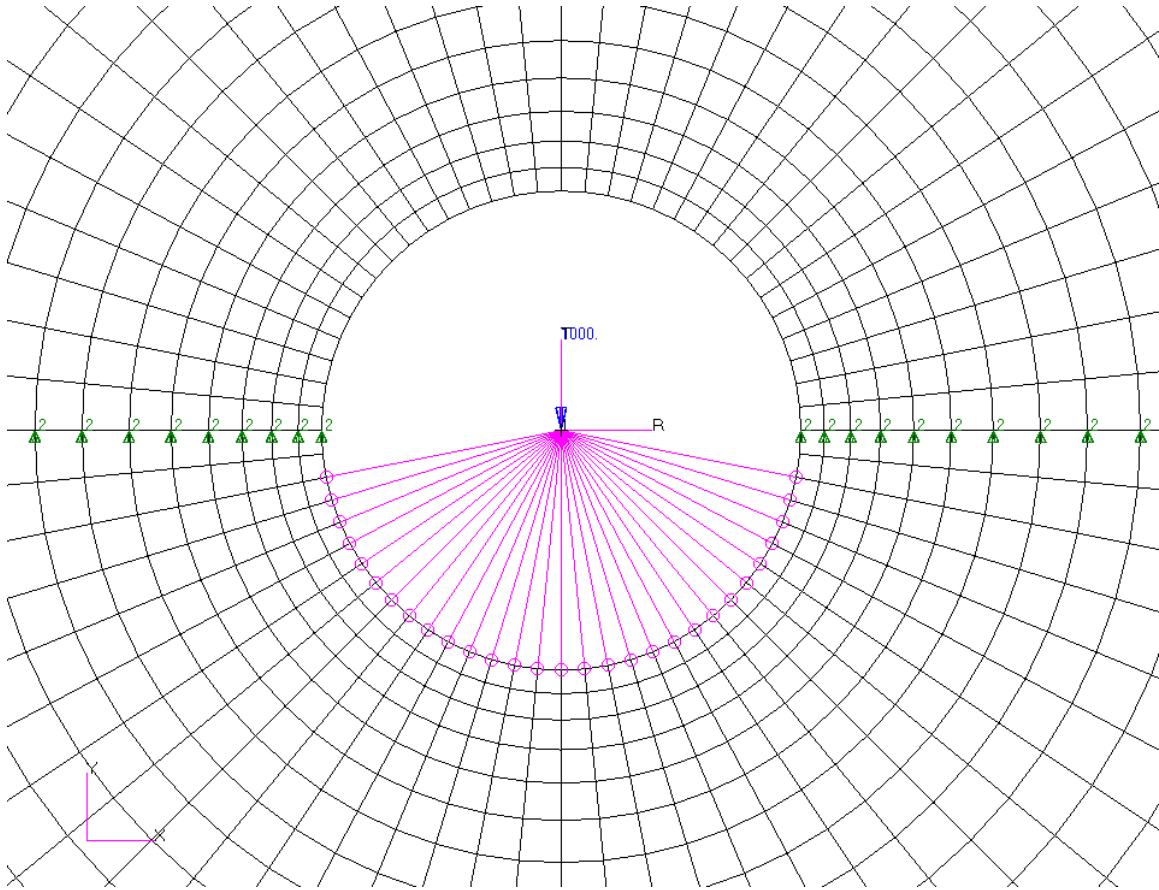


Figure 5. Loading of the Finite Element Model for Metallic Plate Translational Bearing Stiffness Definition.

Table 1. Comparison of the Finite Element and Analytical Results for Translational Bearing Stiffness.

Analysis Method	Translational Bearing Stiffness, <i>lb/in</i>	$\Delta = \frac{S_{analytical} - S_{FEM}}{S_{FEM}} \cdot 100\%$
Finite Element Analysis	1,192,871	-
Et	1,030,000	-13.65
$\frac{Et}{1-\nu^2}$	1,155,875	-3.10

5. Procedure for the Finite Element Modeling and Analysis of Fastener Joints Containing Composite Parts.

Modeling of fastener joints containing composite parts is practically does not differ from described in [1] and [2]. The only difference is in definition of bearing stiffness between composite part and the fastener. The bearing stiffness depends on direction of the resultant load on fastener, which is unknown in the beginning of analysis. Because of this the finite element analysis consists of two main stages:

- Modeling of the fastener joint with calculation of bearing stiffness relatively to the selected fastener coordinate system.
- Iterative finite element analysis with correction of bearing stiffnesses at every step.

The step-by-step procedures for both stages are given in sections below, where we concentrated mainly on the bearing stiffness representation in the joint.

5.1. Finite Element Modeling of the Fastener Joint Containing Composite Parts

Step 1: Determine material properties for each ply for every composite plate in the joint: $E_1^{(i)}$, $E_2^{(i)}$, $G_{12}^{(i)}$, $\nu_{12}^{(i)}$, ply thickness t_i , and coordinates of ply upper z_i and lower z_{i-1} surfaces.

Determine material properties for every metallic plate in the joint: E , ν , and plate thickness t .

Determine compression elastic modulus E_{cf} for the fastener material.

Step 2: Compute the reduced stiffness matrix $Q^{(i)}$ for each ply of every composite plate in the joint using expressions (6) for non-zero components of the matrix.

Step 3: Determine material orientation for each ply (angle θ_i) for every composite plate in the joint relative to the fastener coordinate system.

Positive direction of material principal axes rotation from the fastener coordinate system x - y axes is shown in Figure 3.

Step 4: Compute components $\bar{Q}_{11}^{(i)}$ and $\bar{Q}_{22}^{(i)}$ of the transformed reduced stiffness matrix for each ply of every composite plate in the joint using expressions (2) and (3).

Step 5: For each composite plate - fastener contact compute translational bearing stiffnesses $S_{x_{bt}}$ and $S_{y_{bt}}$ in x and y directions of the fastener coordinate system using formulae (10-a) and (10-b).

Step 6: For every composite plate compute neutral axes coordinates c_x and c_y in planes normal to x and y directions using expressions (11-a) and (11-b).

- Step 7:** For each composite plate - fastener contact compute rotational bearing stiffnesses S_{xbr} and S_{ybr} about x and y axes of the fastener coordinate system using formulae (21-a) and (21-b).
- Step 8:** For each interface of metallic plate and the fastener compute translational and rotational bearing stiffnesses using formulae (25) and (26).
- Step 9:** Build the fastener model using the current procedure [2], with the exception of the CBUSH element properties for fastener locations in composite plates.
- Step 10:** Assign translational and rotational bearing stiffnesses calculated above in x and y directions of fastener coordinate system to corresponding CBUSH elements.

5.2. Iterative Finite Element Analysis

- Step 11:** Run the finite element analysis of the model completed at Step 10.
- Step 12:** From the results of Nastran analysis determine the magnitude and direction Ψ of resultant fastener reaction F at each fastener location in every composite plate (Figure 6).

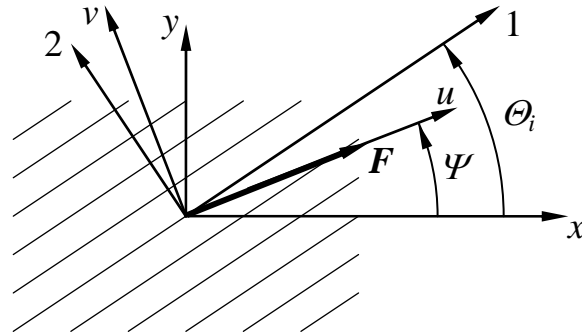


Figure 6. Resultant Fastener Reaction and Direction.

- Step 13:** Re-compute the components \bar{Q}_{11} and \bar{Q}_{22} of the transformed reduced stiffness matrix for each ply of every composite plate for every fastener location in the joint using formulae (2) and (3).

$$\text{Here } m_i = \cos(\theta_i - \psi), \quad n_i = \sin(\theta_i - \psi)$$

- Step 14:** Compute translational bearing stiffnesses in u and v directions for every fastener location in each composite plate.

$$S_{ubt} = \sum_{i=1}^n \frac{t_i}{\frac{1}{\bar{Q}_{11}^{(i)}} + \frac{1}{E_{cf}}} \quad S_{vbt} = \sum_{i=1}^n \frac{t_i}{\frac{1}{\bar{Q}_{22}^{(i)}} + \frac{1}{E_{cf}}}$$

- Step 15:** Compute neutral axes coordinates in planes normal to u and v directions for every fastener location in each composite plate.

$$c_u = \frac{1}{2} \cdot \frac{\sum_{i=1}^n \frac{z_i^2 - z_{i-1}^2}{\frac{1}{\overline{Q}_{11}^{(i)}} + \frac{1}{E_{cf}}}}{S_{ubt}} \quad c_v = \frac{1}{2} \cdot \frac{\sum_{i=1}^n \frac{z_i^2 - z_{i-1}^2}{\frac{1}{\overline{Q}_{22}^{(i)}} + \frac{1}{E_{cf}}}}{S_{vbt}}$$

Step 16: Compute rotational bearing stiffnesses in u and v directions for every fastener location in each composite plate.

$$S_{ubr} = \frac{1}{3} \sum_{i=1}^n \frac{(z_i - c_u)^3 - (z_{i-1} - c_u)^3}{\frac{1}{\overline{Q}_{11}^{(i)}} + \frac{1}{E_{cf}}} \quad S_{vbr} = \frac{1}{3} \sum_{i=1}^n \frac{(z_i - c_v)^3 - (z_{i-1} - c_v)^3}{\frac{1}{\overline{Q}_{22}^{(i)}} + \frac{1}{E_{cf}}}$$

Step 17: Calculate new values of translational and rotational bearing stiffnesses in x and y directions for every fastener location in each composite plate.

Translational bearing stiffness

$$S_{xbr} = S_{ubt} \cos \psi - S_{vbt} \sin \psi \quad S_{ybr} = S_{ubt} \sin \psi + S_{vbt} \cos \psi$$

Rotational bearing stiffness

$$S_{xbr} = S_{ubr} \cos \psi - S_{vbr} \sin \psi \quad S_{ybr} = S_{ubr} \sin \psi + S_{vbr} \cos \psi$$

In reality, during the transformation, coupling bearing stiffnesses S_{xybt} and S_{xybr} appear. They are not taken here into account. However, this inaccuracy is small and becomes even smaller using the iterative process.

Step 18: Assign translational and rotational bearing stiffnesses calculated above in x and y directions of fastener coordinate system to corresponding CBUSH elements at every fastener – composite plate interface.

There is no need to update bearing stiffnesses at fastener – metallic plate interfaces.

Step 19: Re-run the finite element analysis.

Step 20: From the results of latest Nastran analysis determine the magnitude and direction ψ of resultant fastener reaction \mathbf{F} at each fastener location in every composite plate (Figure 6).

Step 21: Compare the results of the latest finite element analysis with results of previous iteration. If the difference between the latest and previous fastener reaction loads for every fastener – composite plate interface is within the established tolerance then the analysis is completed. If the difference at least in one interface is larger than established tolerance then repeat the analysis starting from Step 13.

6. Example Problem.

For an example analysis using the previously described procedure, consider the structure shown in Figure 7. A composite fitting is sandwiched between two aluminum plates, and attached via four protruding head bolts. The fitting is loaded eccentrically by an applied load at the lug on the right side of the fitting. The fasteners transfer this load into the composite plates, which are assumed to be fixed along the top, bottom, and left side.

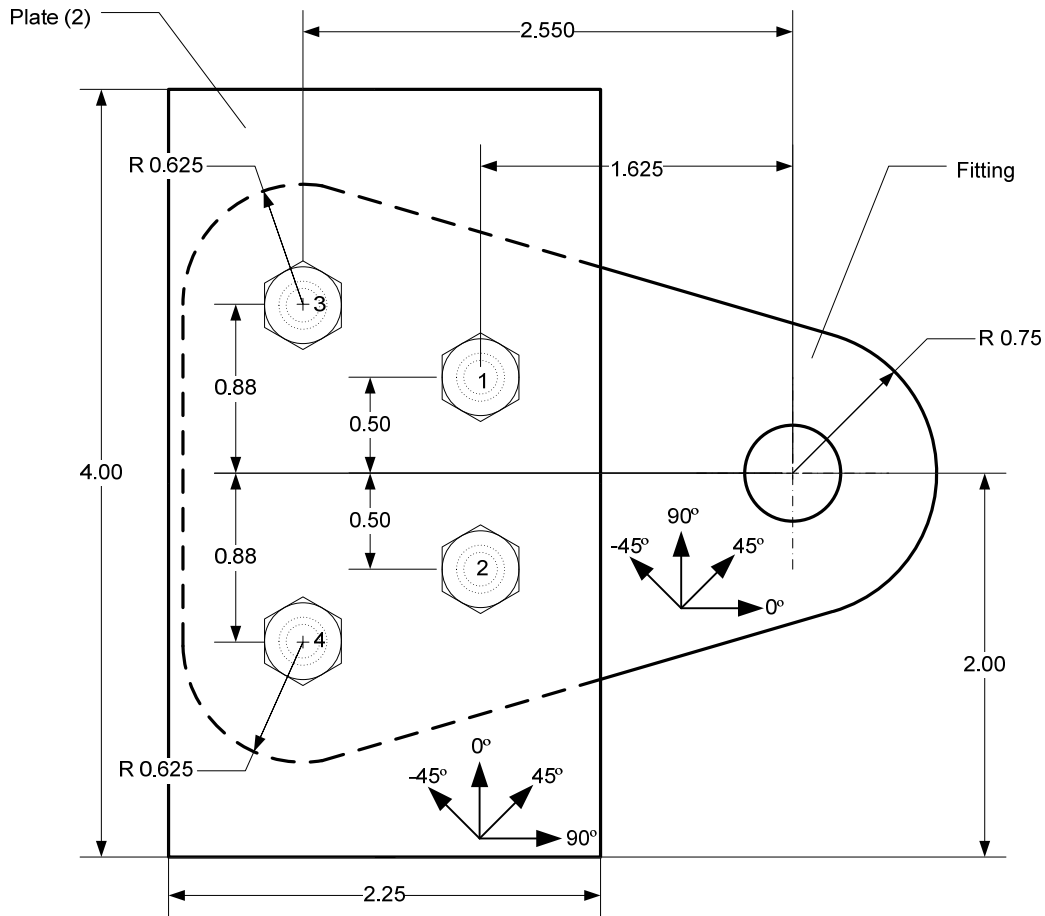


Figure 7. Example Problem Design Configuration.

The composite fitting is assumed to be made up of a generic graphite/epoxy tape material. The lamina material properties of this material are given in Table 2.

Table 2. Graphite/Epoxy Tape Lamina Material Properties.

Material Description	E_1, msi	E_2, msi	ν_{12}	G_{12}, msi	$t_{\text{ply}}, \text{in}$
Graphite/Epoxy Tape	20.6	1.13	0.34	0.58	0.0074

The layup of the fitting consists of 50% 0° fibers (with the 0° direction defined in Figure 7), 40% ±45° plies, and 10% 90° plies. The specific stack up is defined in the following string:

$$[45,-45,0,0,45,0,-45,0,90,0,45,-45,0,0,45,0,-45,0,90,0]_S$$

in which the “S” subscript denotes that the entire stacking sequence is symmetric about the midplane of the laminate. The laminate thus consists of a total of 40 plies, with a total cured ply thickness of the 40 x 0.0074 = 0.296 inches. The aluminum plates are composed of a 0.15 inch thick sheet material.

Using classical lamination theory, the effective engineering constants of the fitting can be computed. These laminate effective engineering constants are given in Table 3.

Table 3. Effective Engineering Constants for Example Laminates.

Layup	E_x, msi	E_y, msi	ν_{xy}	G_{xy}, msi	$t_{\text{laminate}}, \text{in}$
$[(45,-45,0,0,45,0,-45,0,90,0)]_S$	11.98	4.74	0.44	2.46	0.296

Each of the four fasteners in the example problem is assumed to be a 0.25 inch diameter protruding head bolt composed of titanium. The grip length of the fastener is the total thickness of the two plates and the fitting, which is equal to 0.596 inches.

A single loadcase and support condition were considered. A 100 lb load acting downward on the lug hole of the fitting was applied. The composite plates attached to the fitting were fixed along their upper, lower, and leftmost edges, as shown in Figure 8.

A finite element model of the example problem was constructed using MSC Patran. CQUAD4 elements were used to represent the fitting and both plates. The composite properties of the shell elements were established using PCOMP cards. The four fasteners were initially modeled using the Fastener Builder Utility supplied with Patran. The resulting initial model is shown in Figure 9. In this model, the load applied at the center of the lug hole is redistributed to the lower boundary nodes of the hole using an RBE2 element.

Figure 10 shows an isometric view of the finite element model with the top plate removed. This view better illustrates the location of the fastener elements.

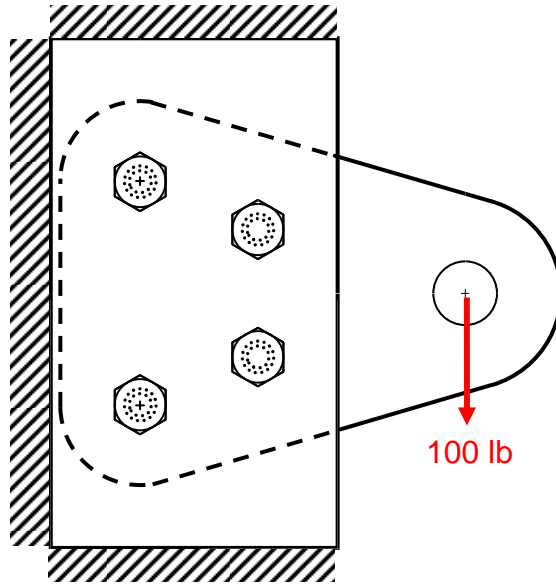


Figure 8. Load Condition Considered for Example Problem.

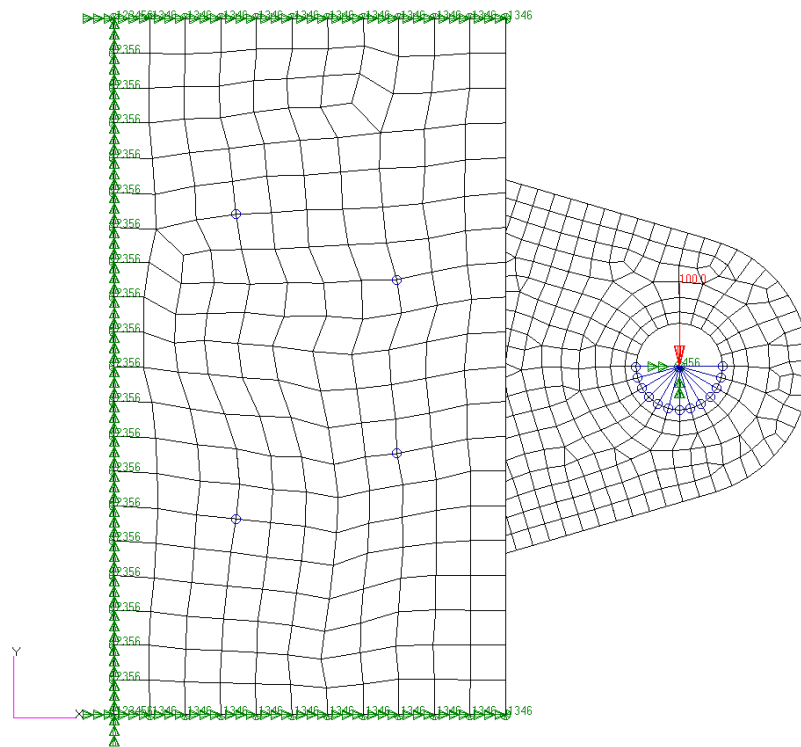


Figure 9. Patran Finite Element Model of the Example Problem.

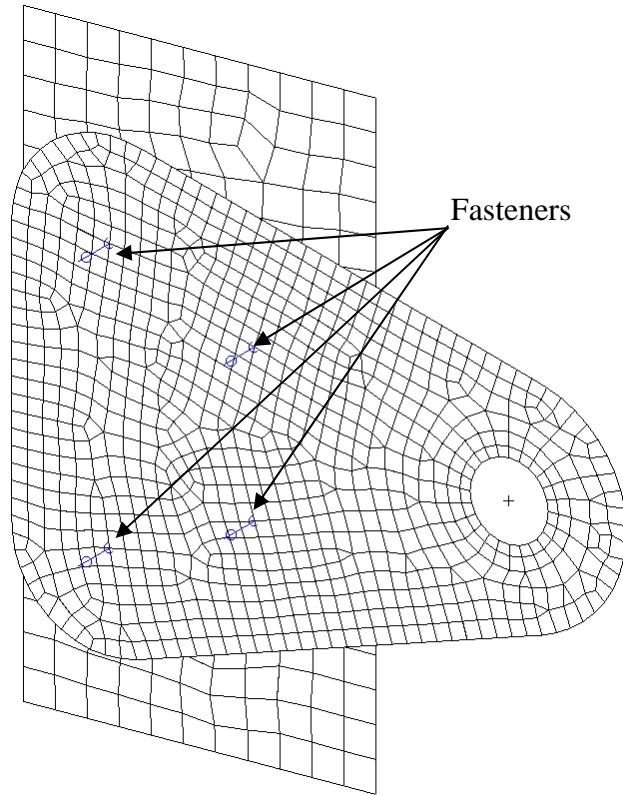


Figure 10. Finite Element Model Showing Fastener Elements.

The stiffnesses used in the CBUSH elements of the fastener models can be pre-computed as a function of the fastener reaction angle. For the CBUSH elements connected to fitting elements, the translational and rotational stiffnesses are shown as a function of load angle in Figure 11. The solid lines show that the translational bearing stiffnesses in the fastener X- and Y-directions are symmetrical – that is, they are exactly equal when the resultant load of the fastener is oriented at 45° to the X-direction. For the rotational bearing stiffnesses, denoted in Figure 11 by the dashed lines, there is a small amount of asymmetry. This asymmetry is due to the use of tape material in the composite fitting. Because the +45° plies are at a slightly different z_i location through-the-thickness of the fitting than the 45° plies, the S_{xbr} and S_{ybr} stiffnesses defined in equation 21 have an asymmetry due to their dependence on z_i .

The initial stiffnesses are chosen with resultant load angles assumed to be 0° relative to global X-direction. In the composite fitting, the initial stiffnesses used for all four fasteners are:

$$S_{xbr} = 1900000 \text{ lb/in}, \quad S_{ybr} = 956000 \text{ lb/in}$$

$$S_{xbr} = 13700 \text{ in lb/in}, \quad S_{ybr} = 6920 \text{ in lb/in}$$

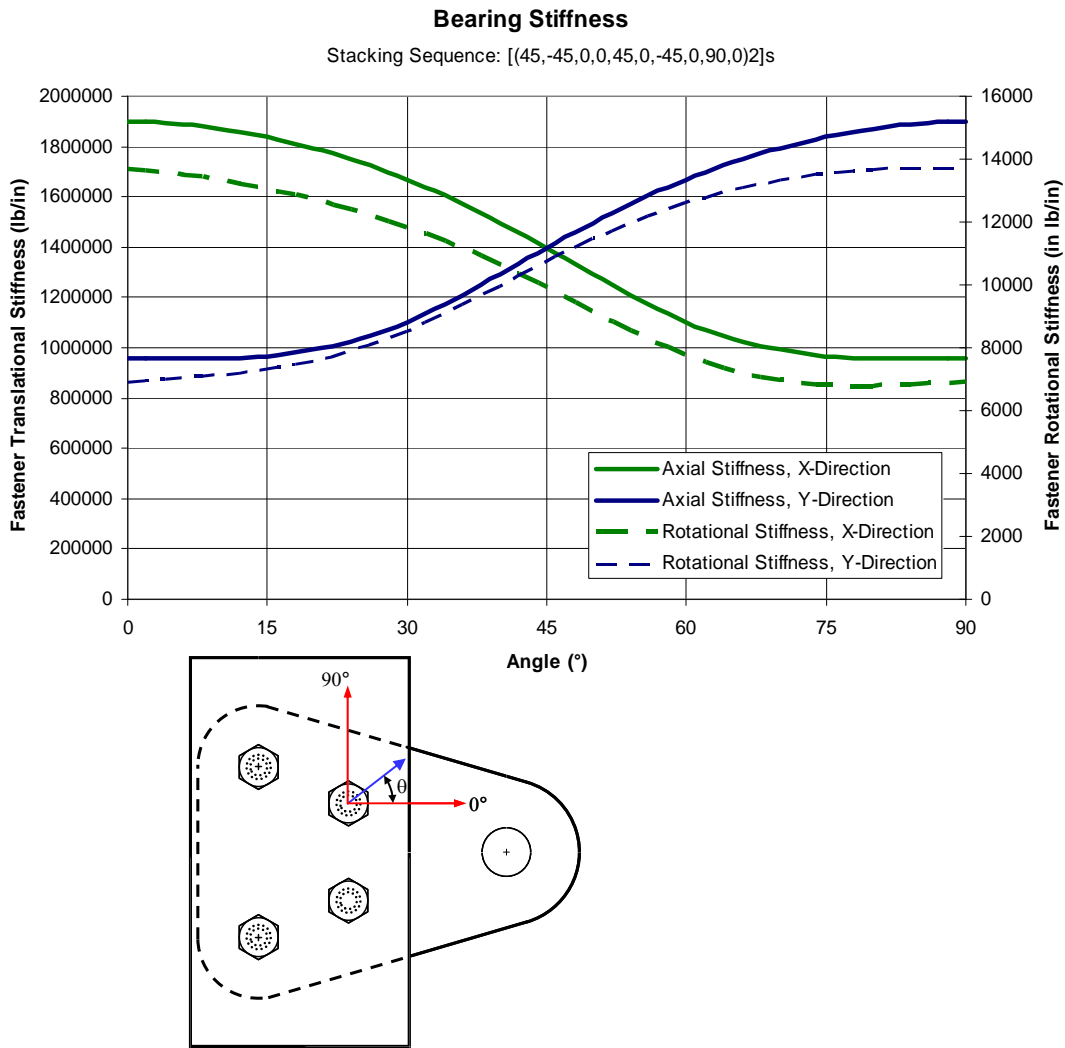
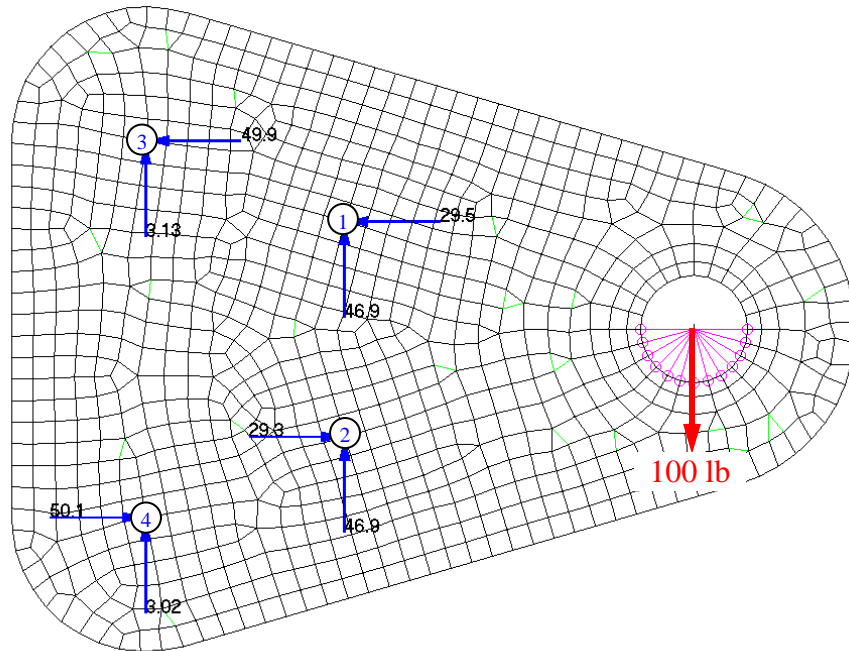


Figure 11. Fastener Translational and Rotational Bearing Stiffnesses in the Composite Fitting as a Function of Angle.

The model was run using the linear static solution of MSC Nastran. The fastener loads acting on the fitting are shown in Figure 12. Based on these results, new fastener stiffnesses were computed in the resultant load direction for each fastener in the fitting. This process was repeated for the upper and lower composite plates.



Fastener ID	R_x, lb	R_y, lb	$\theta, ^\circ$
1	-29.5	46.9	122.2
2	29.3	46.9	58.0
3	-49.9	3.13	176.4
4	50.1	3.02	3.4

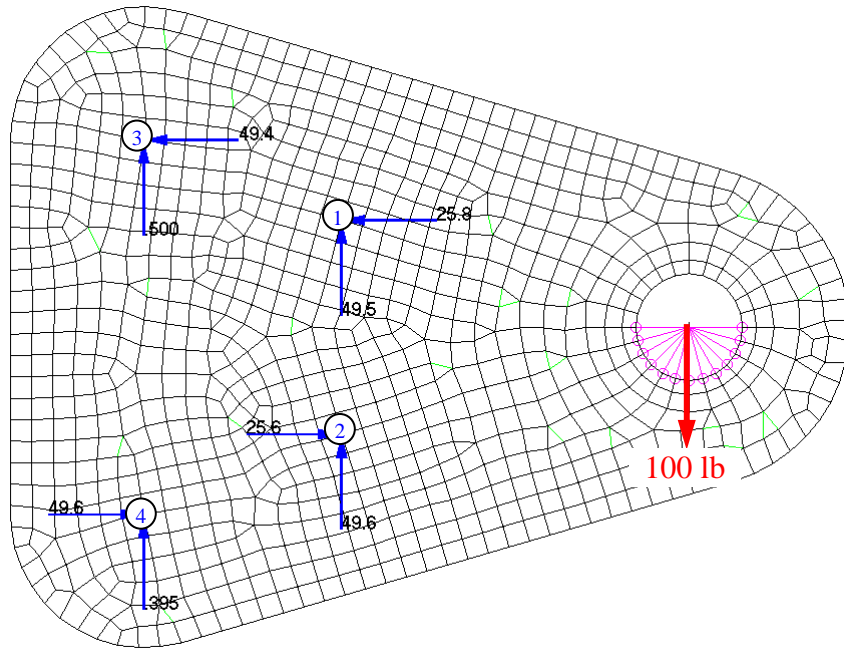
Figure 12. Fastener Resultant Loads in Fitting – Initial Run.

Based on the initial run results, the fitting bearing stiffnesses were modified as shown in Table 4.

Table 4. Fitting Fastener Stiffnesses Modified for Second Run.

Fastener ID	$S_{x_{bt}}, lb/in$	$S_{y_{bt}}, lb/in$	$S_{x_{br}}, in-lb/in$	$S_{y_{br}}, in-lb/in$
1	1140000	1640000	8830	11600
2	1130000	1640000	8000	12400
3	1900000	956000	13700	6850
4	1900000	956000	13600	6980

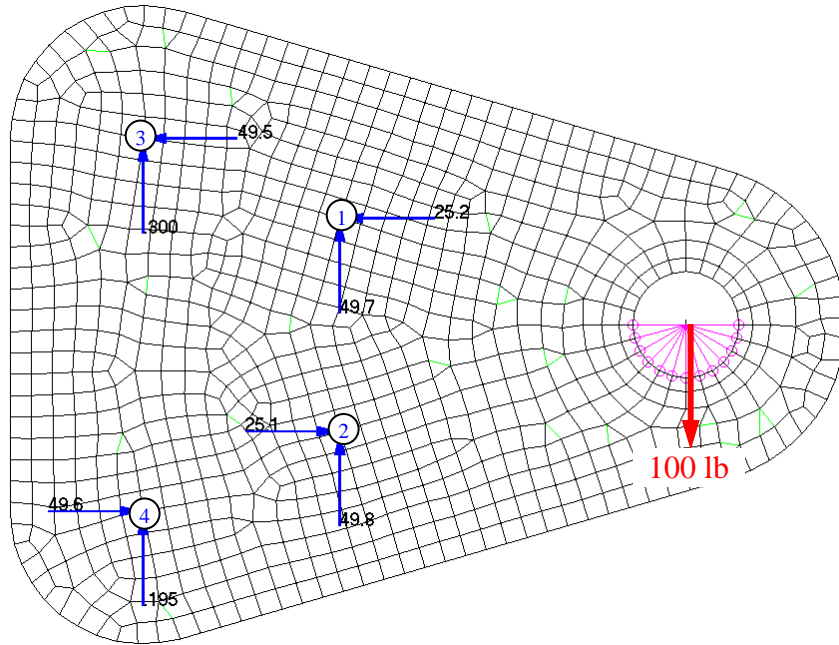
The model was then re-run, and the revised fastener reactions acting on the fitting are shown in Figure 13.



Fastener ID	R_x, lb	R_y, lb	$\theta, ^\circ$
1	-25.8	49.5	117.5
2	25.6	49.6	62.7
3	-49.4	0.50	179.4
4	49.6	0.40	0.5

Figure 13. Fastener Resultant Loads in Fitting – Second Run.

The process of fastener stiffness modification, re-running of the FE model, and re-evaluation of the fastener loads was repeated until the changes in the fastener reactions from run to run were very small. The final fastener reactions, determined after four iterations, are given in Figure 14. This figure shows that the fastener reactions in the fitting converge rapidly for the example problem configuration.



Fastener ID	R_x, lb	R_y, lb	$\theta, ^\circ$
1	-25.2	49.7	116.9
2	25.1	49.8	63.3
3	-49.5	0.30	179.7
4	49.6	0.20	0.2

Figure 14. Fastener Resultant Loads in Fitting – Final Run.

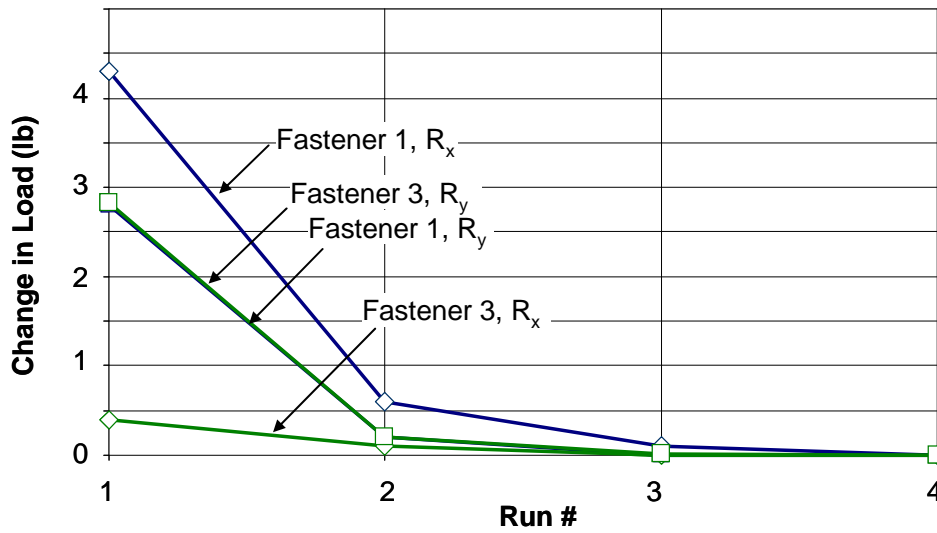


Figure 15. Summary of Fitting Fastener Resultant Loads – Fasteners 1 and 3.

7. Automated PCL Procedure

The PCL utility that currently exists in Patran to automatically generate fastener models was modified to support the creation and analysis of the revised fastener joint model. The PCL procedure was extended to construct fastener models installed in shell elements modeled using PCOMP properties. Bearing stiffnesses were computed using the methods presented in this paper. The main panel of this Patran utility is shown in Figure 16, along with a brief description of the required inputs. This main panel is essentially unchanged in its appearance from the previous utility.

To perform the iterative analysis procedure needed to accurately determine fastener loads, a new analysis action was added to the PCL utility, as indicated in Figure 17. Using this action, Patran automatically iterates the solution of a specific loadcase to minimize the error in fastener reactions due to the variability of bearing stiffnesses as a function of fastener reaction direction. In performing this analysis action, the analyst must specify whether an iterative solution is desired, and if so, what convergence criteria should be used to determine when an acceptable solution has been reached.

8. Conclusion.

The modeling techniques described above for fastened metallic or composite parts represented by shell elements, or metallic parts represented by solid elements, reflect the entire fastened joint behavior including bending, shear, bearing flexibility and compatibility of displacements in the joint. An iterative solution is employed to improve the accuracy of solution of a material having variable bearing stiffness as a function of fastener reaction direction. The modeling approach is presented in terms of MSC.Nastran using CBAR, CBUSH, RBAR, and RBE2 elements and the linear gap techniques; however, it can be applied to another finite element code with similar elements.

References

1. A. Rutman, A. Viisoreanu, J. A. Parady. *Fasteners Modeling for MSC.Nastran Finite Element Analysis*. Paper No. 2000-01-5585. Proceedings of the 2000 World Aviation Conference, San Diego, CA, October 2000.
2. A. Rutman, C. Boshers, L. Pearce, J. Parady. *Fastener Modeling for Joining Parts Modeled by Shell and Solid Elements*. Paper No. 2007-08. Proceedings of the 2007 Americas Virtual Product Development Conference, Detroit, MI, October, 2007.
3. *MSC.Nastran Quick Reference Guide*, 2004, The MacNeal-Schwendler Corporation, Los Angeles, CA
4. Jones, R.M., *Mechanics of Composite Materials*, McGraw-Hill Book Company, New York, 1975
5. Daniel I.M. and Ishai O., *Engineering Mechanics of Composite Materials*, Oxford University Press, New York, 2006

The image shows a software dialog box for creating fasteners. It is divided into several sections, each with a callout box explaining its function:

- Action:** Create (dropdown)
- Option:** Fasteners (dropdown)
- Element and Node ID Control:** Start Elm ID: 1, Start Node ID: 1, Add to Group...: default_group
- Group to which all the Fastener Joint Entities will be Added:** default_group
- Fastener Data:** Diameter, Grip Length, Material..., Plate-to-Plate Contact: Rigid (dropdown)
- Fastener Axis and Alignment:** Symmetry: None (dropdown), Axis List: Coord 0.1, Node Align Tol: Degrees, 5.0, Nudge Node to Axis (checkbox)
- Fastener Locations Defined by Point Representing Fastener (One Point per Fastener):** Select: Points (dropdown), Point List
- Fastener Connections (Defines nodes for Connection):** Select: All Nodes (dropdown), Echo Data (checkbox)

Buttons at the bottom: -Apply-, Cancel

Figure 16. Patran Fastener Creation Utility Input Form.

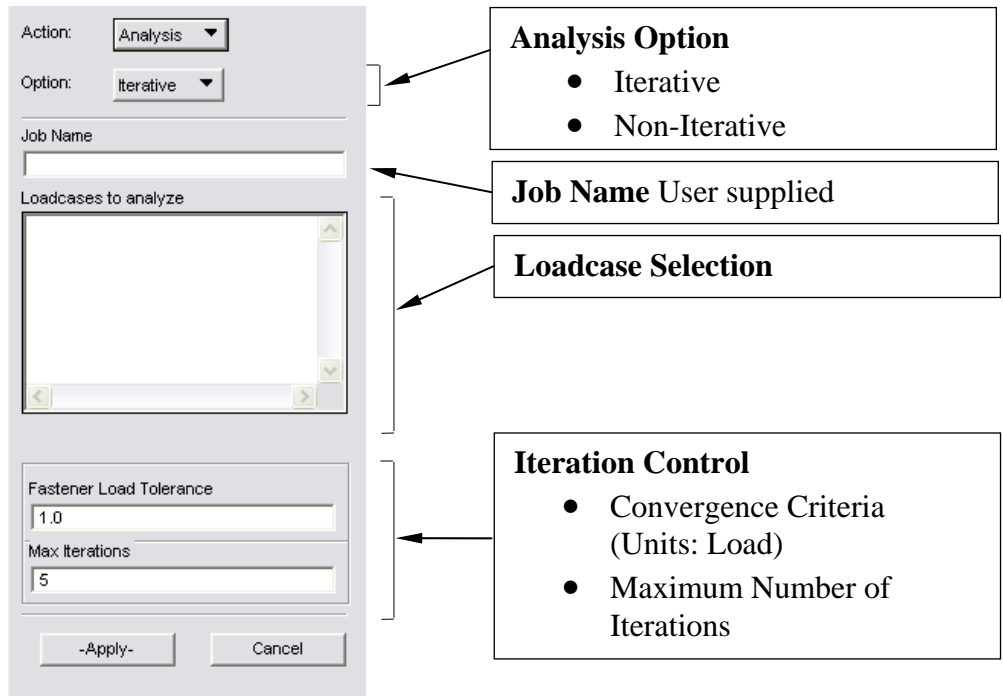


Figure 17. Patran Fastener Creation Utility – Analysis Action for Iterative Solution

For further information please contact:

Alexander Rutman
 316-523-7048
 alexander.rutman@spiritaero.com

John Parady
 817-481-4812, ext. 15
 john.parady@mscsoftware.com

Chris Boshers
 316-523-0374
 chris.boshers@spiritaero.com

Larry Pearce
 770-252-6560
 larry.pearce@mscsoftware.com

Spirit AeroSystems
 P.O. Box 780008
 Mail Zone K78-20
 Wichita KS, 67230
 USA

MSC.Software
 2 MacArthur Place
 Santa Ana, CA 92707
 USA